Technical Report 471

A. R. Dion

Variable-Coverage Communications Antenna for LES-7

17 October 1969

Prepared under Electronic Systems Division Contract AF 19(628)-5167 by

Lincoln Laboratory

MASSACHUSETTS INSTITUTE OF TECHNOLOGY

Lexington, Massachusetts

MASSACHUSETTS INSTITUTE OF TECHNOLOGY
LINCOLN LABORATORY

VARIABLE-COVERAGE COMMUNICATIONS ANTENNA FOR LES-7

A. R. DION

Group 61

TECHNICAL REPORT 471

17 OCTOBER 1969

LEXINGTON MASSACHUSETTS

The work reported in this document was performed at Lincoln Laboratory, a center for research operated by Massachusetts Institute of Technology, with the support of the Department of the Air Force under Contract AF 19(628)-5167.

ABSTRACT

An experimental model of the variable-coverage communications antenna system for the LES-7 spacecraft is described. Consisting of a waveguide lens, a 19-horn feed cluster, and a combiner switch, the system will permit selection of the antenna pattern that best matches a desired coverage on earth. The coverages realizable are of many sizes and shapes, and extend from that of a 3° pencil beam to a full hemisphere. A computer study of this antenna system gave results in good agreement with measurement. The salient features of this study are also described.

Accepted for the Air Force
Franklin C. Hudson
Chief, Lincoln Laboratory Office

CONTENTS

VARIABLE-COVERAGE COMMUNICATIONS ANTENNA FOR LES-7

I. INTRODUCTION

The seventh Lincoln Experimental Satellite (LES-7) will be a synchronous orbit satellite with an X-band communications antenna whose coverage on earth may be modified from ground commands to best meet the requirements of a desired link. Coverage will vary from that of a 3° pencil beam to a full hemisphere, with a large variety of intermediate coverages realizable.

LES-7 will be 3-axis stabilized, with the axis of the communications antenna pointing toward the center of earth. The synthesis technique by which a desired coverage is obtained consists in adding narrow, juxtaposed pencil beams of appropriate phase and amplitude to produce the desired result.[1] A multiple-beam antenna and a multiple-pole, multiple-throw switch (combiner switch) are required for this purpose. The accuracy with which a desired coverage may be synthesized depends upon the beamwidth and the number of pencil-beam elements. The finite aperture of the multiple-beam antenna limits the narrowness of the pencil beams, while their number is limited by efficiency requirements and by the complexity of the associated feed network.

The characteristics of an antenna in a variable-coverage system were studied with computer models for three types of antenna configurations: the paraboloidal reflector with feed cluster, the planar array with two-dimensional Butler feed matrix, and the waveguide lens with feed cluster.

The paraboloidal reflector excited by a feed cluster is unsuitable for a variable-coverage system because of detrimental effects resulting from aperture blockage by the feed structure. Individual narrow beams produced by this configuration ($F/D = 0.6$) do not deteriorate excessively for up to several beamwidths of scan, but the composite earth-coverage pattern, obtained by adding these narrow beams together, shows large gain variation within the coverage. The reason for this behavior is that with all feeds excited with equal amplitude and in-phase to produce an earth-coverage pattern, the illumination on the paraboloid approximates a truncated $J_1(u)/u$ pattern and, therefore, the amount of reflected energy intercepted by the feed cluster is much larger than with single-feed illumination. Reflectors with an offset feed cluster overcome this defect, but the absence of symmetry and the larger size of such antennas make them unattractive for the present application.

Planar arrays fed with two-dimensional Butler beam-forming matrices (called Butler arrays) have been investigated both theoretically and experimentally.[2] Results obtained with an 8×8 array of square horn elements have shown this configuration to be suitable for a variable-coverage antenna system. However, one drawback of this configuration is the inherent loss of the beam-forming matrix. The matrix developed for this system is of stripline construction

and exhibits an insertion loss of 2.0 dB which is believed to represent well the state of the art for this component. The efficiency of single-beam generation by the Butler array is correspondingly reduced. When the Butler array is used to form a composite beam (for instance, an earth-coverage pattern), the losses are the same as for single-beam operation, as opposed to a reflector or lens system where losses due mainly to spillover are reduced by the resultant arraying of the feed elements.

Lenses illuminated by a feed cluster are well suited for variable coverage systems. The absence of aperture blockage and the ability to scan several beamwidths off-axis without excessive pattern degradations favor this configuration. In particular, the waveguide lens can be made very lightweight and highly reliable and, therefore, is appropriate for spacecraft applications. This report is devoted to an investigation of a waveguide lens and feed-cluster antenna designed to meet the requirements of the LES-7 communications antenna. Figure 1 is a photograph of an experimental model of this antenna. Measurements performed with this model will be shown to compare well with the results of a concurrent computer investigation. A brief description of a combiner switch proposed for this antenna is also reported. Aside from its application as a special-purpose communications antenna, this configuration suggests itself as a feed for highly efficient large Cassegrainian antennas. A discussion of this application concludes the report.

II. WAVEGUIDE LENS

The use of waveguide lenses for microwave antenna applications has been reported by various authors.[3-5] In particular, Ruze[3] has demonstrated the wide-angle scanning capability of cylindrical metal-plate lenses designed to have two focal lines. Waveguide lenses exhibiting two focal points may also be designed as shown by the following analysis. Referring to Fig. 2, it is required to determine the shape of the two surfaces of a waveguide lens such that rays issued from a point source S located in the XOZ plane and displaced from the lens axis by $f \sin\alpha$ will, after refraction by the lens, form a plane wave whose direction of propagation is that of the line joining the source to the center of the lens. Mathematically, this condition is satisfied by equating the path length of a general ray to that of the central ray. By letting $d(x, y)$ be the length of a general waveguide and d_o that of the central waveguide, and $\mu = \lambda/\lambda_g$ be the index of refraction, the path-length equation is

$$[(x - f \sin\alpha)^2 + y^2 + (z + f \cos\alpha)^2]^{1/2} + \mu d(x, y) = f + \mu d_o - x \sin\alpha$$
$$+ [z + d(x, y) - d_o] \cos\alpha \quad . \tag{1}$$

After some manipulations, this equation becomes

$$x^2 \cos^2\alpha + y^2 + z^2 \sin^2\alpha + 2xz \sin\alpha \cos\alpha = \{[d(x, y) - d_o] (\cos\alpha - \mu)\}$$
$$\cdot \{[d(x, y) - d_o] (\cos\alpha - \mu) + 2(f - x \sin\alpha + z \cos\alpha)\} \tag{2}$$

Since there are two unknowns (the position and length of a waveguide), an infinite number of solutions exists. Imposing the condition that the lens be symmetrical with respect to the YOZ plane, i.e., that two focal points exist, yields another equation obtained by replacing x by $-x$ in Eq. (2), with $d(-x, y) = d(x, y)$, giving

$$x^2 \cos^2 \alpha + y^2 + z^2 \sin^2 \alpha - 2xz \sin\alpha \cos\alpha = \{[d(x,y) - d_o] (\cos\alpha - \mu)\}$$

$$\cdot \{[d(x,y) - d_o] (\cos\alpha - \mu) + 2(f + x \sin\alpha + z \cos\alpha)\} \quad . \tag{3}$$

Subtracting Eq. (3) from Eq. (2), we find

$$d(x,y) - d_o = -z \cos\alpha / (\cos\alpha - \mu) \tag{4}$$

while adding Eqs. (2) and (3) and substituting Eq. (4) gives

$$x^2 \cos^2 \alpha + y^2 + z^2 + 2fz \cos\alpha = 0$$

which can be written in the form

$$\frac{x^2}{f^2} + \frac{y^2}{f^2 \cos^2 \alpha} + \frac{(z + f \cos\alpha)}{f^2 \cos^2 \alpha} = 1 \quad . \tag{5}$$

Equation (5) is the mathematical expression of a spheroid whose trace in the XOZ plane is

$$\frac{x^2}{f^2} + \frac{(z + f \cos\alpha)^2}{f^2 \cos^2 \alpha} = 1 \tag{6}$$

i.e., an ellipse with foci at the two-point sources, and whose trace in the YOZ plane is

$$y^2 + (z - f \cos\alpha)^2 = f^2 \cos^2 \alpha \tag{7}$$

i.e., a circle of radius $f \cos\alpha$.

Letting z_1 and z_2 be the z-coordinates at the input and output, respectively, of a general waveguide, we have

$$z_2 = z_1 + d(x,y)$$

$$= \frac{-z_1 \mu}{\cos\alpha - \mu} + d_o \quad .$$

Substituting $z_1 = z$ from Eq. (5) yields

$$\frac{x^2}{f^2} + \frac{y^2}{f^2 \cos^2 \alpha} + \left[\frac{z_2 - d_o}{\mu/(\cos\alpha - \mu)} - f \cos\alpha\right]^2 = 1 \tag{8}$$

as the equation of the outer face, i.e., an ellipsoid of unequal semi-axes. The two-focus lens is thus double-concave and axially asymmetric.

For small off-axis beam deviations, as is the case for the LES-7 antenna, where the maximum scan angle is 8.66° (half the cone angle subtended by the earth at the synchronous satellite), a two-focus design differs negligibly from that obtained by allowing the two foci to merge together on the axis of the lens. Under this condition, the lens becomes of axial symmetry, the surface facing the feed is a segment of a sphere centered at the feed, while the opposite surface is a segment of a spheroid. Since this lens is a limiting case of a two-focus design, it may be expected to exhibit a better scanning performance than that of lenses with appreciably different surface shapes. Evidence of this behavior will be given in Sec. VI of this report. In addition, concave surfaces allow for a more efficient aperture illumination than do flat or convex surfaces.

The waveguide lens is a two-dimensional, nonplanar array of waveguide radiators and, therefore, its radiation characteristics may be computed by application of array theory and concepts. A computer program was developed to evaluate these characteristics. Necessarily, the computer model required several approximations to be made. In particular, the element pattern of a waveguide radiator within the lens environment was taken to be that of an identical isolated radiator except as described below.

In general, it is necessary to step (or zone) the lens to reduce its thickness and to increase its bandwidth. A step in the lens is made where the lens thickness exceeds $\lambda/(1-\mu)$, which is the length of a waveguide for which the path length is one wavelength shorter than under free-space propagation. The lens may be stepped on either (or both) of its surfaces. However, steps on the surface opposite the feed appear preferable in order to reduce shadowing effects.

Stepping the lens has some disadvantages, however, as lower efficiency and unequal E- and H-plane beamwidths result. Steps form flat surfaces in which nearby waveguide radiators are mirrored, thus modifying the directional patterns of these radiators. This effect is accounted for in the computer analysis of the waveguide lens which is described in Sec. III below.

An experimental investigation of the characteristics of a waveguide lens, designed in accordance with the previous analysis, yielded results that agreed well with the computer predictions. A photograph of the experimental lens was presented in Fig. 1; a dimension drawing is shown in Fig. 3. The lens, made of square waveguide, is intended for use with circularly polarized waves. However, all measurements reported herein were carried out with linearly polarized waves.

The waveguide width (i.e., the index of refraction) affects the maximum thickness of a lens as well as the quantity of waveguide elements required to fabricate a lens. The larger the waveguide width the thicker is the lens, but the smaller is the quantity of waveguide elements required. In addition, the amount of reflected energy at the lens surface increases as the waveguide width is made smaller; on the other hand, waveguide widths sustaining higher mode propagation must be avoided. TE_{10} and TE_{01} are the dominant waves in square waveguides. The first higher-order waves are TE_{11} and TM_{11}, both having the same cutoff wavelength $\lambda_c = \sqrt{2}a$, thus setting an upper limit of 0.7 for the index of refraction. The lower limit of the index is determined by the amount of tolerable reflection loss. In practice, index values in the range 0.55 to 0.65 appear most desirable. It will be shown in Sec. V that the lens bandwidth is not very sensitive to the index of refraction within this range of values.

The F/D ratio determines the number of zones in a lens which, in turn, affects efficiency and bandwidth; the larger this number, the smaller are the efficiency and bandwidth. (However, zoned lenses have greater bandwidths than unzoned lenses). An F/D ratio of 1 was required to meet the LES-7 bandwidth requirements.

III. COMPUTED RADIATION CHARACTERISTICS

The radiation characteristics of the lens are calculated by summing the far-field contribution of each waveguide radiator. Amplitude, phase, and the radiation pattern of each radiator are obtained under the following conditions:

(a) The effects of reflections at the surfaces of the lens are neglected.

(b) The power incident on each waveguide propagates through the waveguide in the dominant modes.

(c) The radiation pattern of each waveguide radiator is the same as that of an identical radiator in free space except for radiators adjacent to a step where it is modified as described below.

Let the lens be illuminated by a feed of known radiation characteristics and consider the system as a transmitting antenna. The amplitude and phase of the field at the input to each waveguide are computed from the feed characteristics and from the geometry of the system. The value of the field at the output of each waveguide radiator is equal to its value at the input modified by the insertion phase of each waveguide.

The radiation pattern of each waveguide radiator, assumed to be that of the isolated open waveguide, is broad and does not affect the lens radiation pattern in axial and near-axial directions. However, the radiation pattern of waveguide radiators adjacent to a step is substantially modified by reflections on the step surface, and the resultant effect on the lens pattern is appreciable.

Consider a cross section of the lens in the vicinity of a step as shown in Fig. 4. Waveguides of reduced length reflect in the flat surface formed by the wall of the longer unstepped waveguides, thus altering the element pattern of these radiators. Consider the case where the field is polarized perpendicular to the step surface as shown in Fig. 4(a). Rays issued from a waveguide radiator and reflected from the surface add in phase with direct rays to produce an element pattern resembling somewhat that illustrated. The beamwidth of this element pattern is appreciably smaller than that of a general radiator, and little power is radiated in direction behind the surface of a step. In the case where the field is polarized parallel to the surface of a step, reflected rays add out-of-phase with direct rays to produce a resultant element pattern typically as shown in Fig. 4(b). Little power is radiated in directions parallel to the surface of a step as well as behind this surface. In addition, for this latter sense of polarization the length of a waveguide immediately adjacent to a step is effectively longer than its design value due to the parallel plate formed by the outer walls of contiguous waveguides, thus causing a phase error to exist at these waveguide apertures.

Zoning a lens has some deleterious effects on the radiation characteristics, however, the principal one being a reduction of efficiency since radiation in the forward direction is greatly reduced for certain radiators. A secondary effect is to make the H-plane beamwidth larger, and the E-plane beamwidth smaller, than in the absence of zoning. The computer calculations of the lens radiation characteristics assume the radiation pattern of waveguide radiators adjoining a step to be identical to that of an open waveguide parallel and in contact with an infinite ground plane. The effect of a step on waveguide radiators further removed from the step is greatly reduced by the directivity of each radiator and is neglected in the computation.

The calculations are obviously limited to applications where the previous approximations hold reasonably well. Fortunately, this is the case over the range of angles and frequencies of concern in the present application. An example of this is shown in Figs. 5(a) and (b) where computed E- and H-plane patterns of an axial beam are compared with measurements. The center feed of a feed cluster, described in Sec. IV below, was excited to generate this beam. Agreement in the E-plane is excellent. The discrepancy in the H-plane may be attributed in most part to the small displacement between E- and H-plane phase centers of the primary radiation, as refocusing brought closer agreement of the H-plane patterns with a corresponding deterioration of agreement of E-plane patterns.

As predicted, the beamwidth in the E-plane is smaller than in the H-plane. Computed efficiency also agrees well with measurements. Since the feed provides for an illumination taper of only 5 dB, efficiency is appreciably reduced by spillover. Improved efficiency would result from the choice of a higher directivity feed. However, in a multiple-feed system the feed dimensions are determined by system requirements which, usually, do not lead to optimum efficiency.

IV. FEED CLUSTER

The feed-cluster geometry is determined by the required crossover level of adjacent beams and by the total coverage desired. The higher the crossover level, the smaller is the corresponding spacing between feeds and, therefore, the smaller is the area available for a feed aperture. Reducing feed apertures leads to increased spillover with correspondingly smaller efficiency. In addition, the composite patterns formed by adding several or all the narrow beams together must meet certain requirements. For instance, the earth-coverage pattern for LES-7 must meet requirements with regard to uniformity of gain over the earth's surface as well as on the boundary. These requirements also affect the feed-cluster design.

To determine the effect of the feed-cluster parameters on the secondary radiation characteristics, the single-feed, waveguide-lens computer program was modified to include multiple-feed illumination. The modified program allows computation of any single-beam pattern as well as of patterns resulting from the addition of several or all the beams together. Feed clusters with square and with triangular spacing arrangement, and with different feed spacings, were studied. The feed cluster shown in Fig. 6 was chosen as best meeting the system specifications. It consists of 19 conical horns located at the intersection of a triangular lattice; the horns are spaced 2 inches apart and their aperture is also 2 inches in diameter. A photograph of the experimental feed cluster is presented in Fig. 7.

The radiation patterns of individual feeds of the feed cluster showed little variance from one another. Figure 8 shows the E- and H-plane patterns of the center horn. Since the lens angular aperture is 60°, an illumination taper averaging about 5.2 dB is deduced. Mutual coupling between feeds is negligible, the largest measured value being −42 dB.

Figures 9 and 10 are lens radiation patterns obtained when typical elements of the feed cluster are excited. The feed elements terminology is shown in Fig. 6. Each element is designated by two indices: the first corresponds to its row number, and the second to its position in a row. Radiation patterns of the axial beam (3,3) were shown earlier in Fig. 5. Figure 9 shows the H-plane pattern of the beam generated when horn 3,1 is excited, while Fig. 10 is the E-plane pattern corresponding to excitation of horn 1,2. Computed patterns also shown in these figures agree satisfactorily. Figure 11 shows the superimposed H-plane patterns of the five beams of the center row. Beam offset angles are equal to the feed offset angles, and crossover levels are about 4.5 dB. Measurements of the gain of each of the 19 beams showed a maximum variation of ±0.5 dB, with an average gain of 31.5 dB. The cross-polarized component of the field shows a few lobes some −26 dB below the normal component and is everywhere else much smaller.

The radiation patterns obtained by exciting all the feeds in phase and with equal amplitude to produce an earth-coverage pattern are shown in Figs. 12(a) and (b). (A power divider, consisting of a center-fed radial waveguide terminated on equally spaced terminals along its periphery, was used to divide the power equally and in phase among the 19 feed horns. The uniformity of power and phase at the output terminals was ±0.2 dB and ±2°, respectively.) Computed patterns, also shown in Fig. 12, agree satisfactorily with experimental values. A measured contour plot of the earth-coverage beam is given in Fig. 13. Gain ripple is about 2 dB peak-to-peak, and the average gain is 21.5 dB. The ideal earth-coverage pattern is a right-circular cone subtending the earth at the satellite; its directivity is 22.5 dB. The synthesized earth-coverage pattern approximates closely this ideal pattern. The 1-dB loss of gain may be shown to be due, in most part, to grating lobes of the feed cluster. These grating lobes are observed in the planes $\phi = 0°$

and ±60°, and point at an angle of about 55° from the axis. In the planes $\varphi = \pm 60°$, the grating lobes are 12 dB below the peak of the composite secondary pattern, while in the plane $\varphi = 0°$ they are down 20 dB from this peak. The grating lobes and the earth-coverage beam have about the same beamwidth.

The previous considerations suggest that slightly more directive feeds are physically realizable for the feed cluster. Feeds with a gain about 1 dB larger than the experimental feed gain would provide the necessary directivity to eliminate the grating lobe. A corresponding increase of the secondary pattern gains could be expected. Since each feed aperture occupies an area almost equal to the maximum area available for each feed, increased-gain feeds can only be obtained by resorting to end-fire elements such as dielectric rods, yagis, helices, or periodically loaded structures.

V. BANDWIDTH

Since waveguides are highly dispersive, the bandwidth of a waveguide lens antenna is small. A formula for the bandwidth, obtained by setting the maximum allowable phase error to $\pi/4$, and reproduced from Silver,[4] is

$$\text{bandwidth} \approx \frac{25}{2 + K} \text{ percent}$$

where K is the number of zones, counting the zone on axis as the first. The designed lens has three zones and, therefore, a corresponding bandwidth of 5 percent. However, in a zoned lens the phase error does not increase monotonically as a function of radial distance, but follows a stepwise increase, and the effect of such error distribution on the secondary pattern must be obtained and the bandwidth determined from criteria applied to the results. The gain of the lens antenna as a function of frequency was computed for this purpose and the results are plotted in Fig. 14. This computation was carried out for excitation by the center feed of the feed cluster and also includes the effect of frequency on the feed characteristics. Calculations made for two values of the index of refraction show that bandwidth increases with index values closer to unity; however, the difference is small for practical values of this index. Redefining the bandwidth as the 1-dB width of the gain-loss-vs-frequency curve yields a bandwidth of about 15 percent. Radiation patterns at frequencies 5 percent above and below the design frequency are given in Figs. 15(a) through (d). The principal effect of frequency deviations on radiation patterns is to raise the level of the first lobe ring and to fill in the first null ring.

Operation of the lens at frequencies off the design frequency gives rise to a stepwise quadratic phase error distribution in the aperture. Such error distribution may be canceled out, in most part, by refocusing of the feed. In other words, the focal length is a function of frequency. Computer calculations of focal length vs frequency gave the results shown in Fig. 16. The focal length was taken as the separation between the center of the lens and an axial feed resulting in maximum gain at a given frequency. For an unzoned lens the focal length variation must follow the expression for thin optical lenses[6] or

$$F = F_o(1 - \mu_o)/(1 - \mu)$$

where F_o is the focal length at the design index of refraction μ_o. Substituting $\mu = [1 - (\lambda/2a)^2]^{1/2}$ for a waveguide lens gives the focal length variation expressed in Fig. 16 for unzoned lenses. As expected, the focal length excursion is smaller for the zoned lens, i.e., the zoned lens has greater bandwidth.

The bandwidth of a waveguide lens antenna could be increased by exciting it with a feed whose phase center varies with frequency such as to reduce the focusing errors. End-fire radiating elements exhibiting this property are conceivable.

VI. MAXIMUM SCAN ANGLE

The waveguide lens and feed cluster described above involved a maximum beam offset of only two beamwidths for which little pattern deteriorations were observed to result. For the sake of interest, radiation characteristics were computed for much larger offset angles; the amplitude distribution in the aperture was assumed to be axially symmetric and to taper quadratically to −10 dB on the edge. Thus, only phase errors arising from offsetting the feed contribute to computed pattern degradations. The scanning surface for the computations is a segment of a sphere whose center coincides with the center of the lens. This surface was verified to be the locus of nearly optimum gain as a function of feed offset. Radiation patterns corresponding to feed offset angles of 0°, 10°, 20°, and 25° are shown in Fig. 17. Pattern deteriorations are relatively small up to a feed offset angle of about 20°. However, a significant broadening of the beam is observed as the feed offset is increased. By setting the limit of scan as the offset angle corresponding to a gain reduction of 1 dB, it is concluded that a 3° beam may be scanned about seven beamwidths from broadside. For smaller values of beamwidth, scanning over a larger number of beamwidths will result. However, the correspondence between these two variables has not been studied.

The lens, it is recalled, is double-concave with one surface being a segment of a sphere. Since this lens is a special case of a two-focus lens design, it was expected to exhibit better scanning properties than lenses devoid of a spherical surface. That this is the case was verified in the particular instance of a plano-concave lens for which radiation characteristics were computed for parameter values identical to those of the double-concave lens. Figure 18 shows the results which, when compared with Fig. 17, indicate the appreciably larger coma lobe associated with the plano-concave lens. It should be recognized, however, that computations are based on assumptions that are increasingly dubious as the feed offset angle increases and, therefore, actual behavior may depart appreciably from that predicted for those angles.

VII. COMBINER SWITCH

The LES-7 communications antenna generates 19 narrow beams, each one illuminating a different sector of the earth's hemisphere. In order to excite any of these beams or any combinations of these beams, a special switching system is required to connect the transmitter or receiver to the feed cluster. The combiner switch being developed for this application is illustrated in Fig. 19. A corporate feed with a variable power divider at each junction divides the power among the 19 feeds in any desired ratio. In general, equal power is required at each feed, but the number of feeds to be excited and their location is determined by the required coverage.

The power divider at each junction may be realized in several ways. The differential-phase-shift power divider illustrated in Fig. 20 was chosen for the present application. It consists of two 3-dB hybrids joined by two interdependent 90° phase shifters. Power applied to the sum terminal of the magic tee splits between the two outputs of the 3-dB, sidewall coupler according to the relations shown in the illustration. The insertion phase of the power divider is independent of the power split ratio and, ideally, no power is reflected at the input terminal.

VIII. DISCUSSION

The multiple-feed waveguide lens antenna was shown to perform efficiently in a variable-coverage system. Obviously, this antenna is also suitable for switched pencil-beam systems. Worthwhile performance improvements would seem realizable through the use of appropriate end-fire elements for the feed cluster. The behavior of this antenna is predictable with reasonable accuracy over a range of angles equal to several beamwidths. Only the limiting cases represented by the narrow-pencil beams and the earth-coverage beam have been considered in this report. A large variety of intermediate sizes and shapes are realizable. As an example, Fig. 21 is the computed contour plot obtained when horns 5,1, 5,3, 4,4 and 1,2 are excited. The plot superimposed on an orthographic projection of the western hemisphere shows coverage of the continental United States, of part of western Europe, and of the southern tip of South America. The antenna system makes use of only 19 beams, but systems with several hundred beams appear realizable with this technique.

The synthesized earth-coverage pattern was shown to match quite well the ideal pattern, i.e., a right-circular cone subtending the earth at the satellite. This behavior suggests another practical application for the multiple-feed waveguide lens configuration. As a feed for very large aperture Cassegrainian antennas, this configuration would lead to higher efficiencies than heretofore realized, since nearly all the power radiated by this feed would be uniformly distributed over the subreflector – only a very little amount being spilled over. The further requirement of a spherical wavefront is equally well satisfied; the computed deviation from this surface is only ±0.01 wavelength over the extent of the synthesized beam. In addition, since the field incident upon a given sector of the secondary reflector may be controlled by adjusting the phase of the field radiated by the corresponding feed of the feed cluster, a practical way of electronically compensating for surface profile errors is derived. Such techniques have been proposed and tested for a one-dimensional system.[7,8] The multiple-feed waveguide lens is a practical approach to the two-dimensional case.

ACKNOWLEDGMENTS

The mechanical design of the waveguide lens and feed cluster was skillfully carried out by D.G. Golder. Dr. L.J. Ricardi contributed stimulating and valuable discussions and also provided the concept for the combiner switch.

REFERENCES

1. L. J. Ricardi, private communication.
2. J. B. Rankin, "Two-Dimensional 64-Element X-band Butler Array" (unpublished notes).
3. J. Ruze, "Wide-Angle Metal Plate Optics," Proc. IRE 38, 53 (January 1950).
4. S. Silver, Microwave Antenna Theory and Design, M.I.T. Radiation Laboratory Series, Vol. 12 (McGraw-Hill, New York, 1948), pp. 402-412.
5. G. C. Southworth, Principles and Application of Waveguide Transmission (Van Nostrand, New York, 1948), pp. 459-470.
6. M. Born and E. Wolf, Principles of Optics (Pergamon Press, Oxford, 1959), p. 162.
7. D. E. N. Davies and A. W. Rudge, "Some Results of an Electronic Compensation for Surface Profile Errors in Parabolic Reflectors," Electron. Letters 4, No. 20, 433 (4 October 1968).
8. A. W. Rudge and M. J. Withers, "Beam-Scanning Primary Feed for Parabolic Reflectors," Electron. Letters 5, No. 3, 39 (6 February 1969).

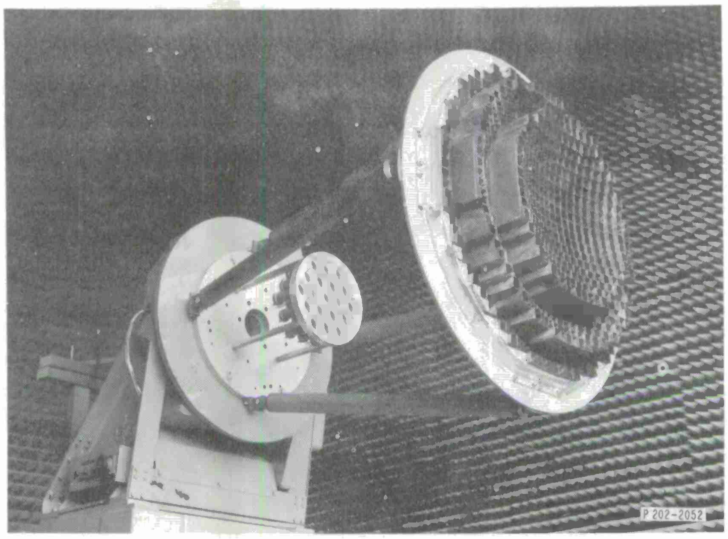

Fig. 1. Experimental lens antenna on antenna test mount.

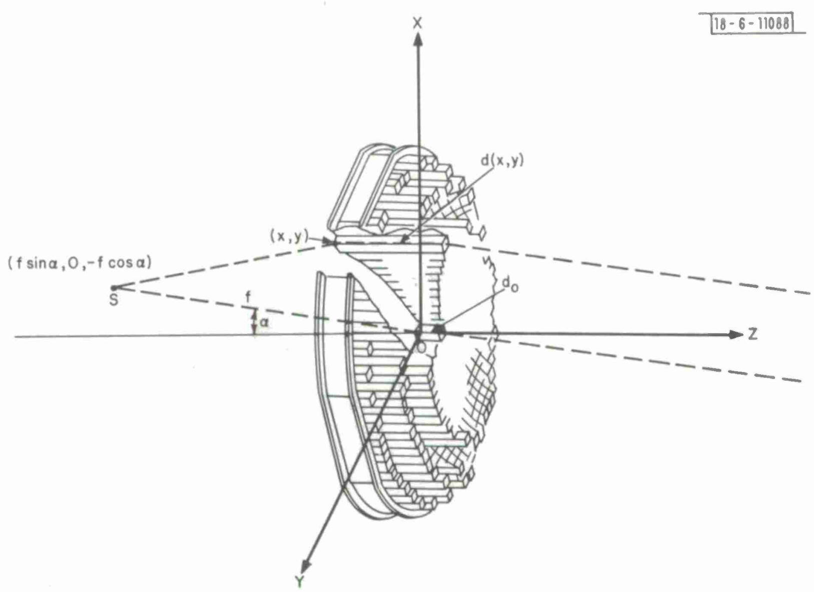

Fig. 2. Coordinate system.

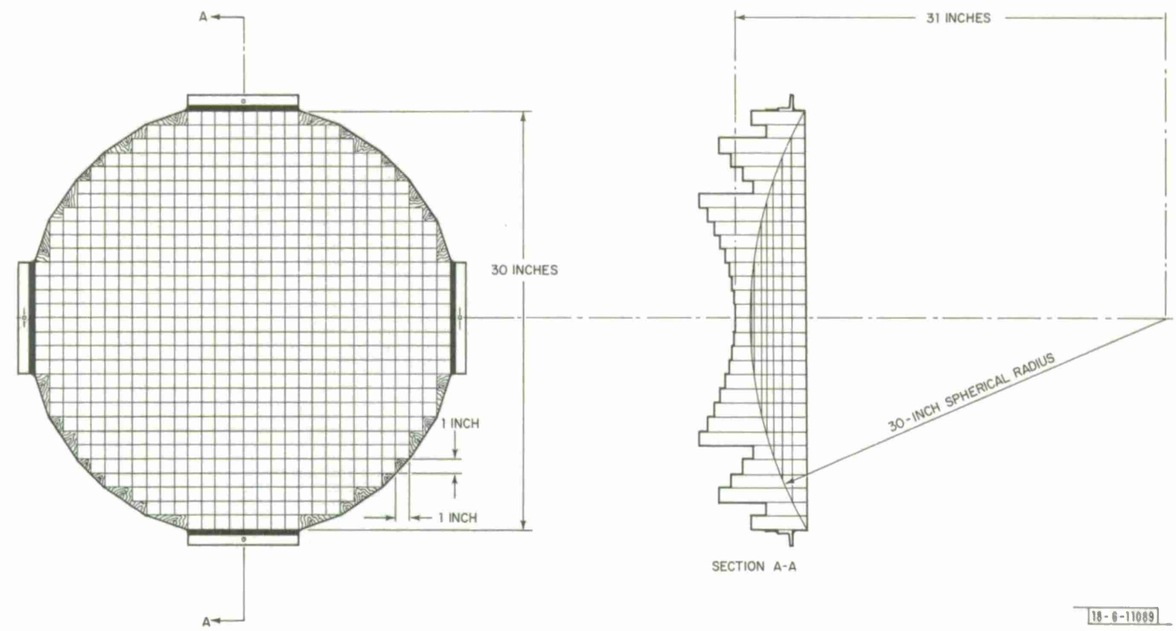

Fig. 3. Lens dimensions.

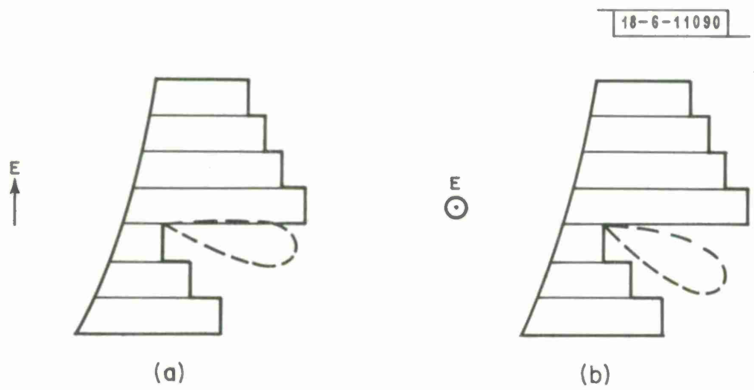

Fig. 4. Effect of step on element pattern: (a) step perpendicular to electric field, and (b) step parallel to electric field.

(a)

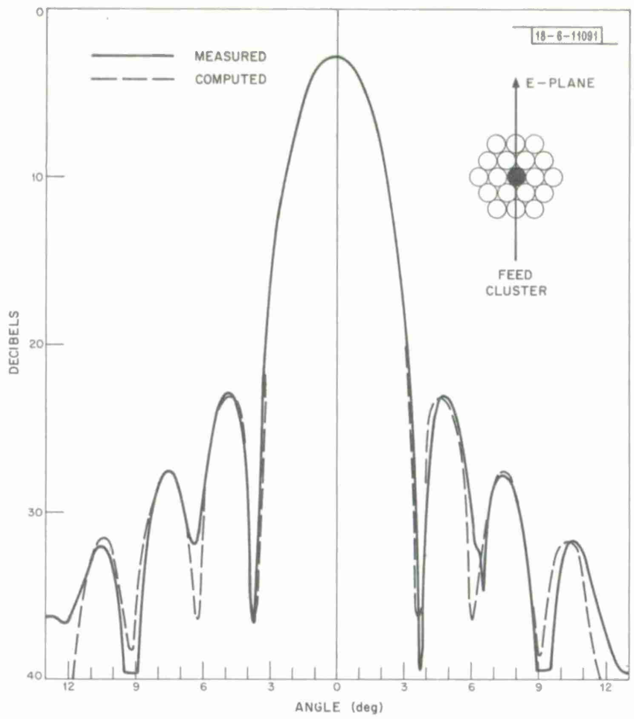

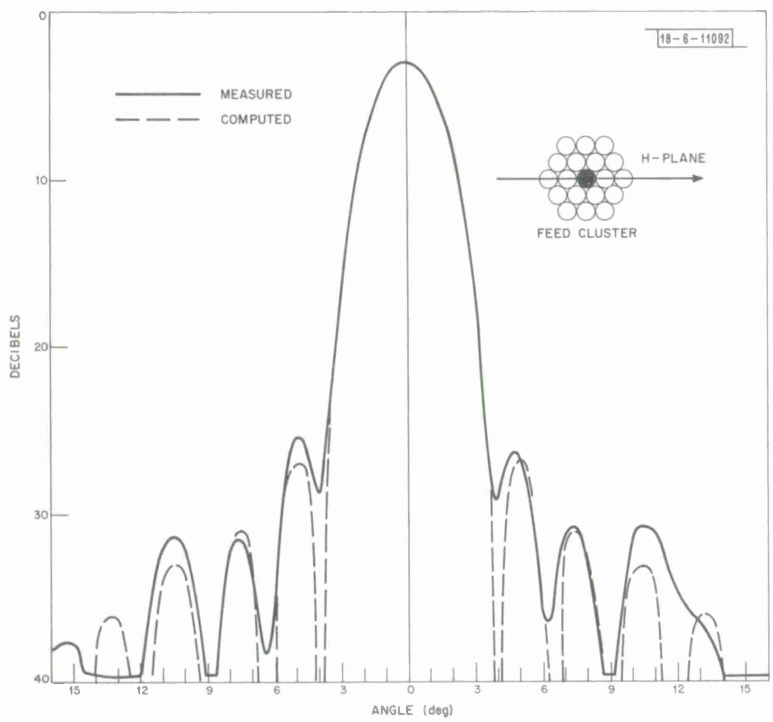

(b)

Fig. 5. Radiation patterns of axial beam at design frequency: (a) E-plane, and (b) H-plane.

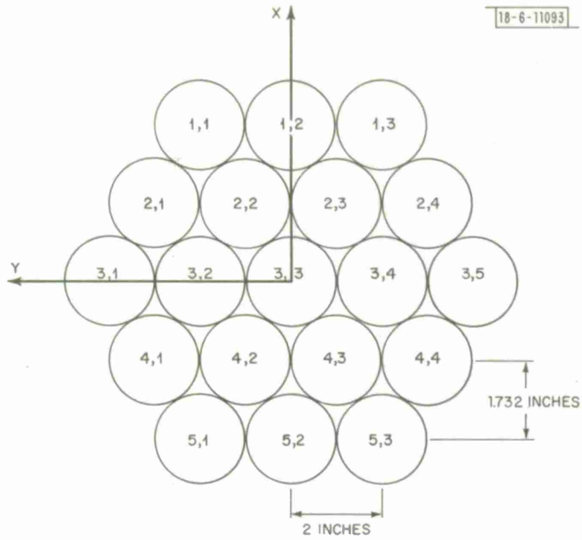

Fig. 6. Geometry and terminology of feed cluster.

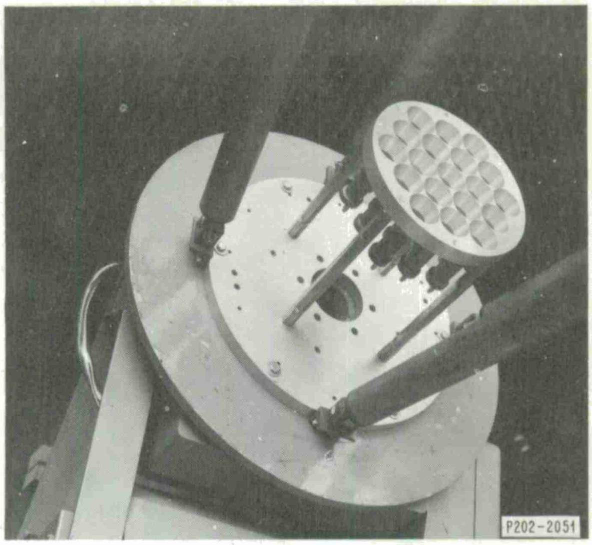

Fig. 7. Photograph of feed cluster.

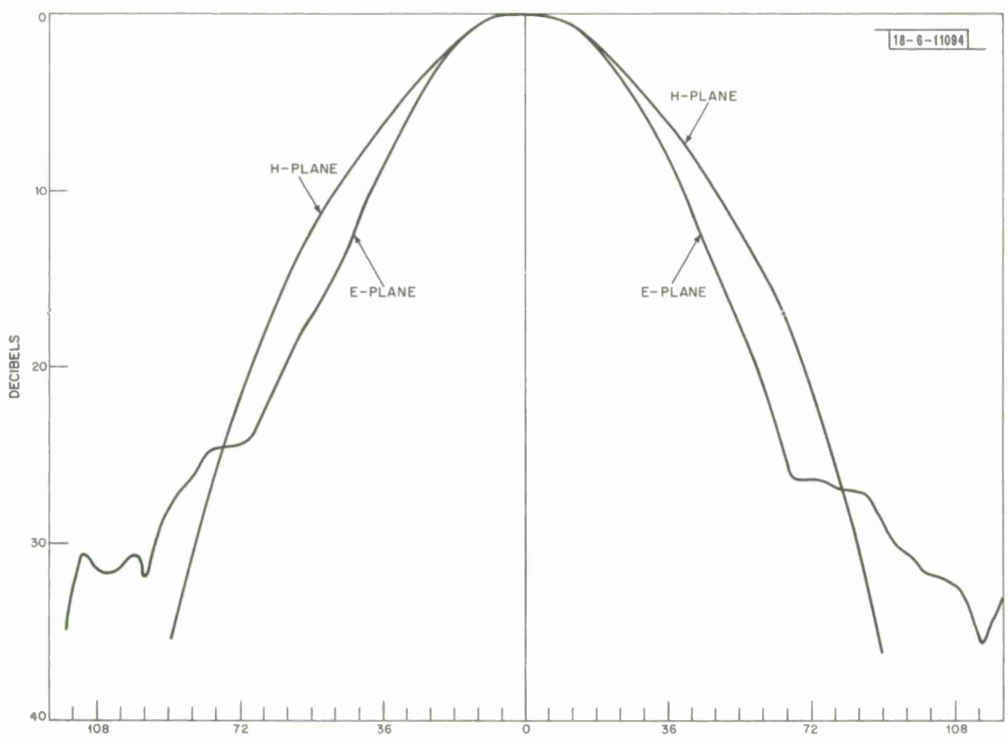

Fig. 8. Primary E- and H-plane radiation patterns of center horn of feed cluster.

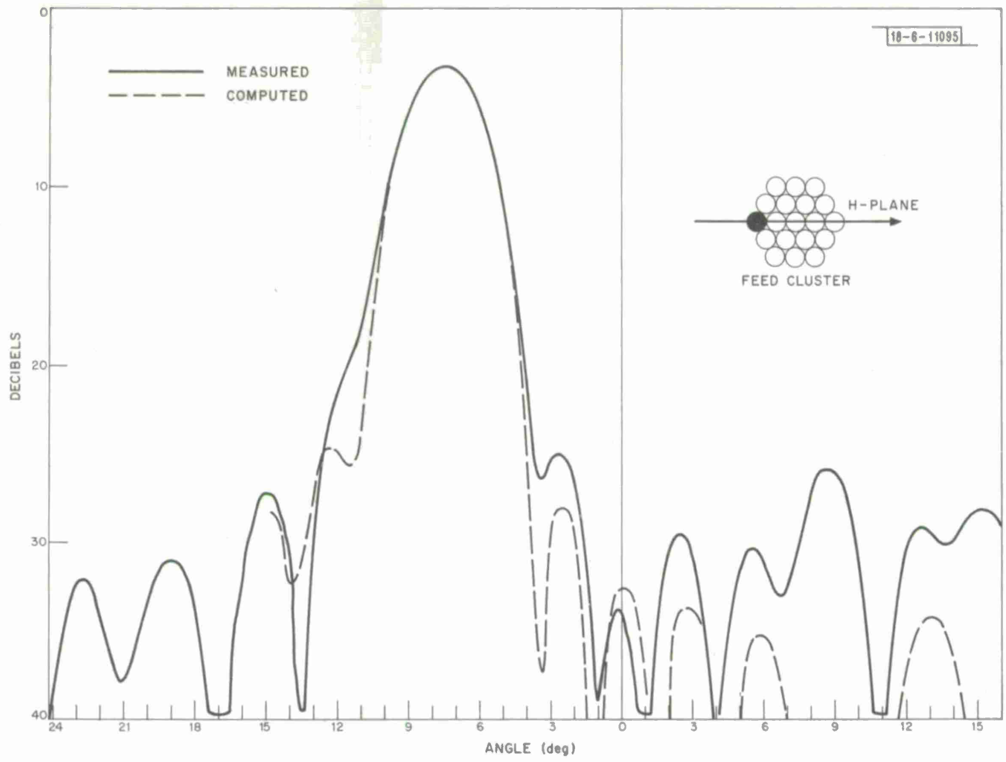

Fig. 9. H-plane pattern of beam 3,1 at design frequency.

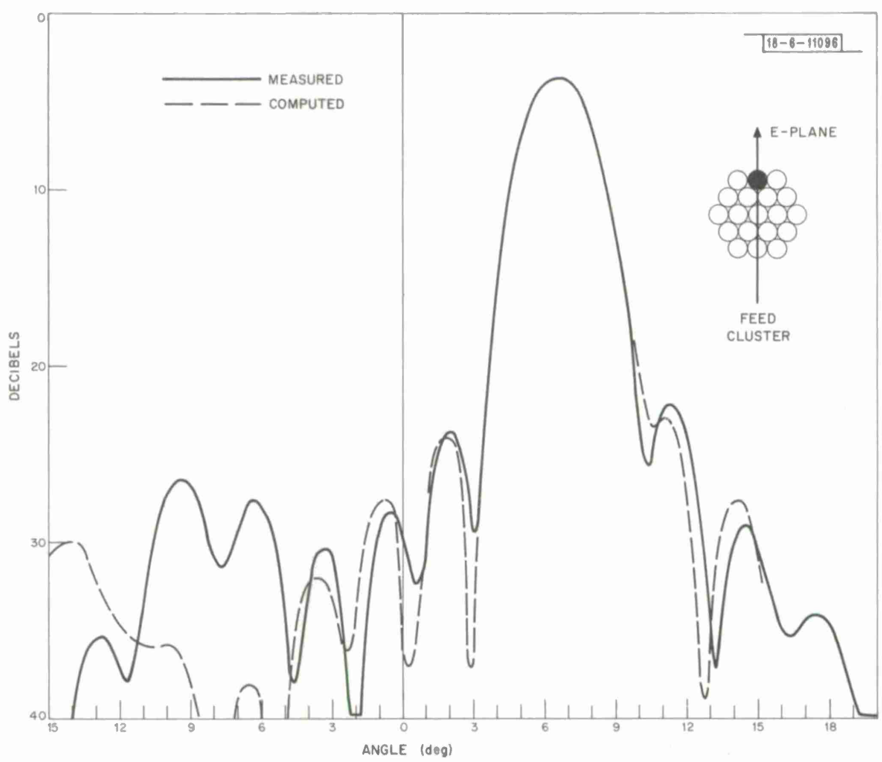

Fig. 10. E-plane pattern of beam 1,2 at design frequency.

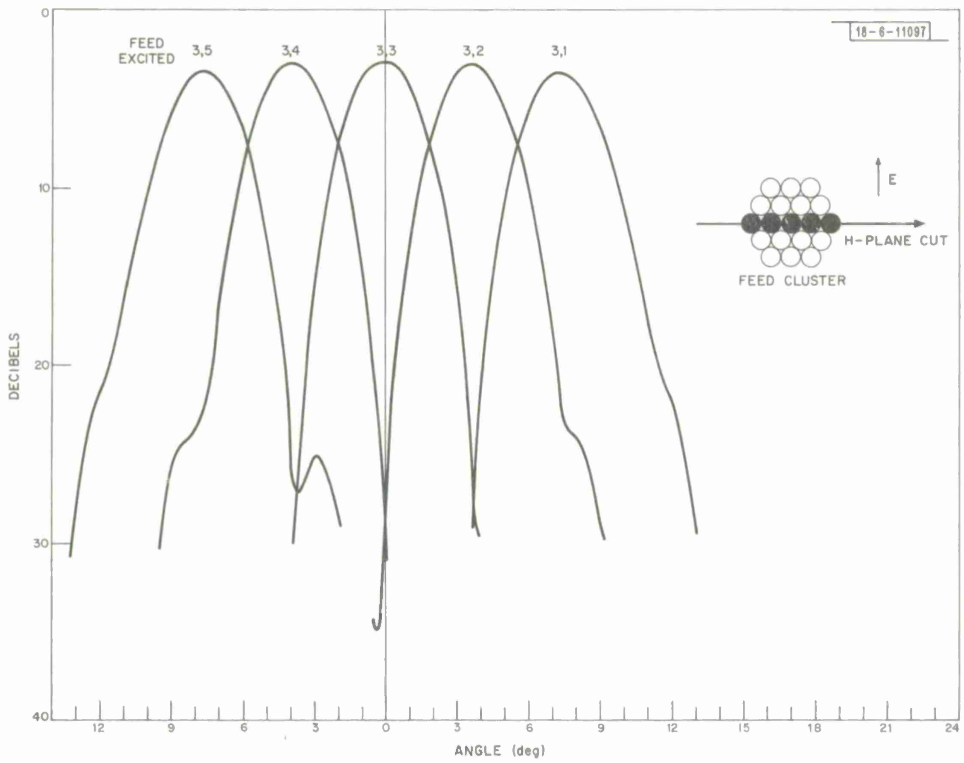

Fig. 11. Superimposed H-plane patterns of center row beams. Measured at design frequency.

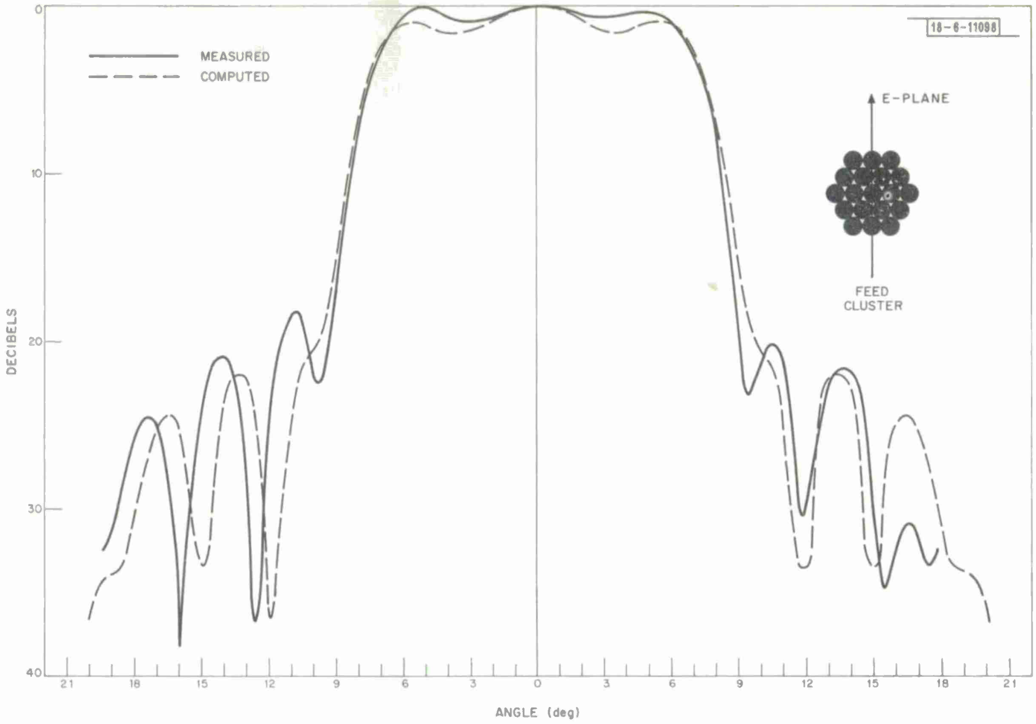

(a)

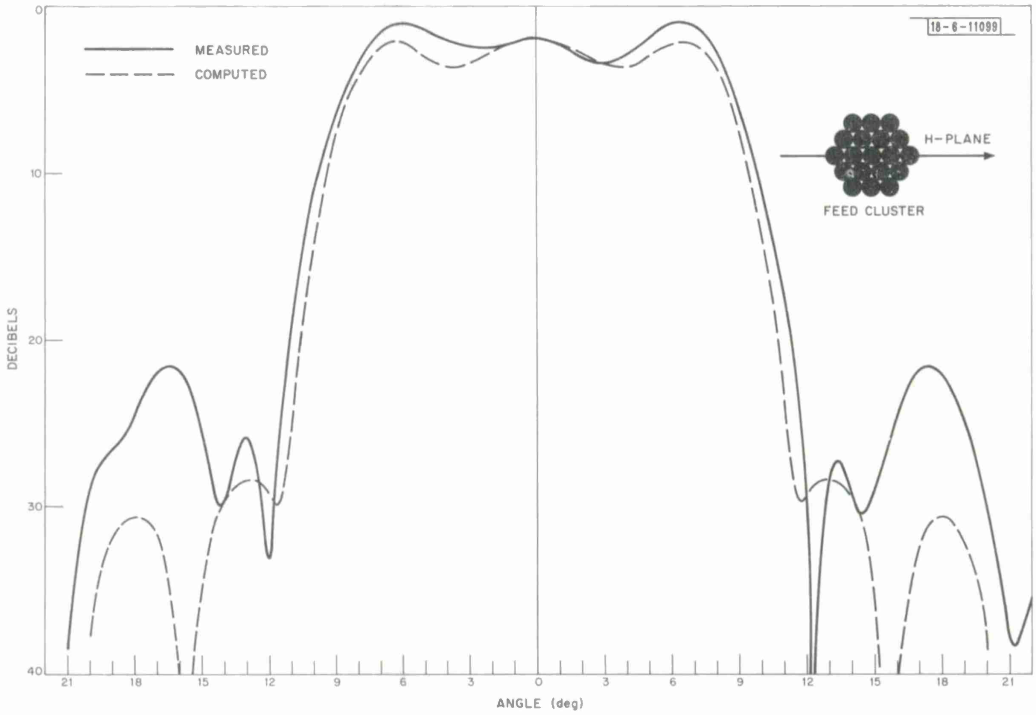

(b)

Fig. 12. Earth-coverage patterns: (a) E-plane, and (b) H-plane at design frequency.

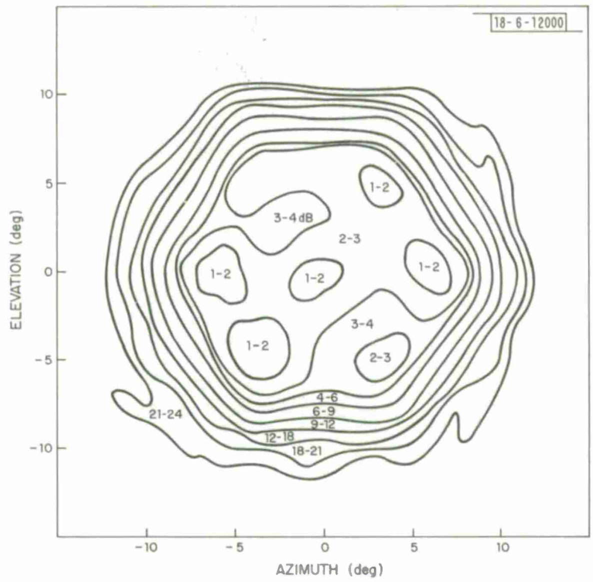

Fig. 13. Measured contour plot of earth-coverage beam at design frequency. Power level is in decibels.

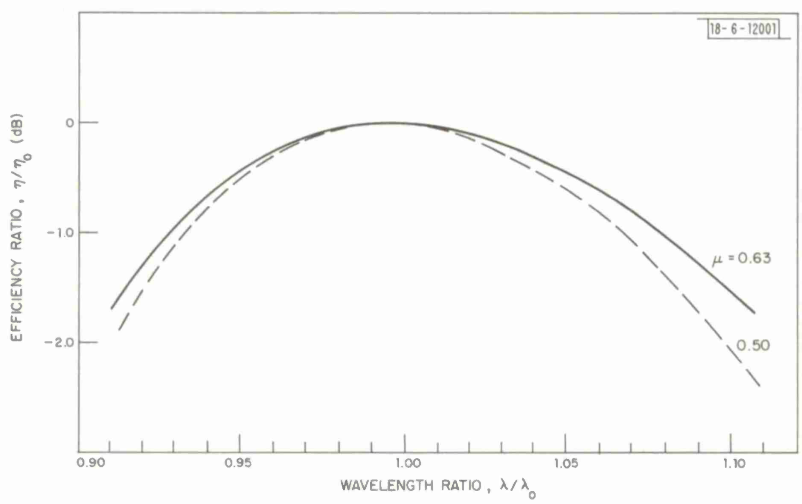

Fig. 14. Computed gain of lens antenna as a function of frequency.

(a)

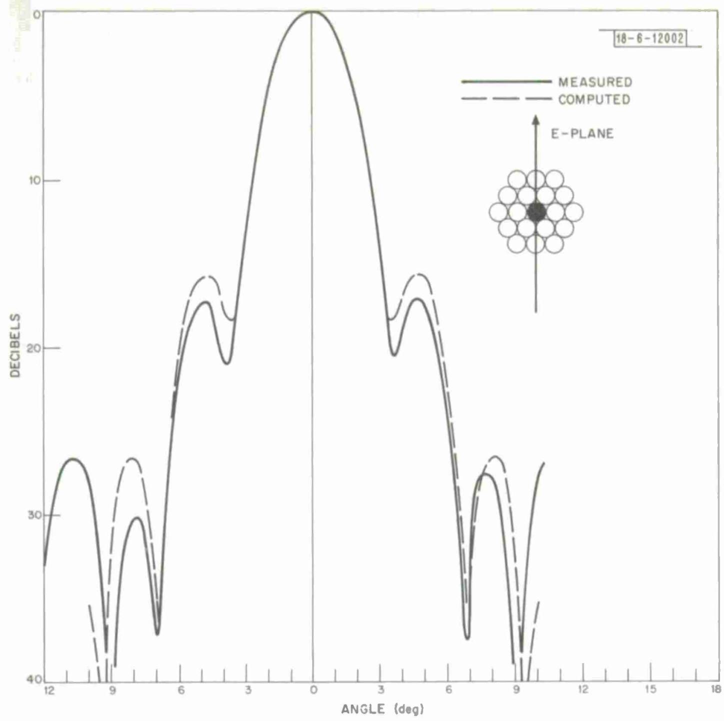

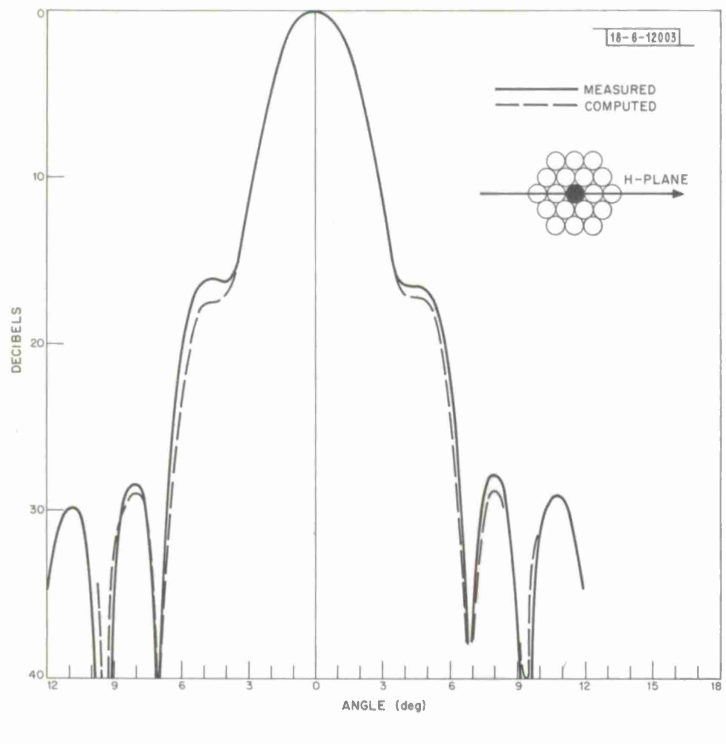

(b)

Fig. 15. Radiation patterns of axial beams at frequencies 5 percent below and above design frequency: (a) E-plane and (b) H-plane, 5 percent above; (c) E-plane and (d) H-plane, 5 percent below.

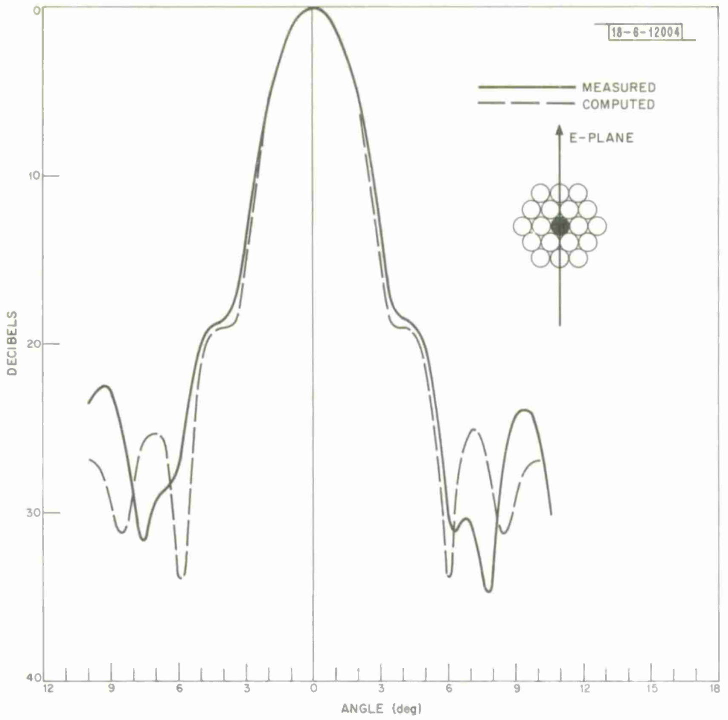

(c)

(d)

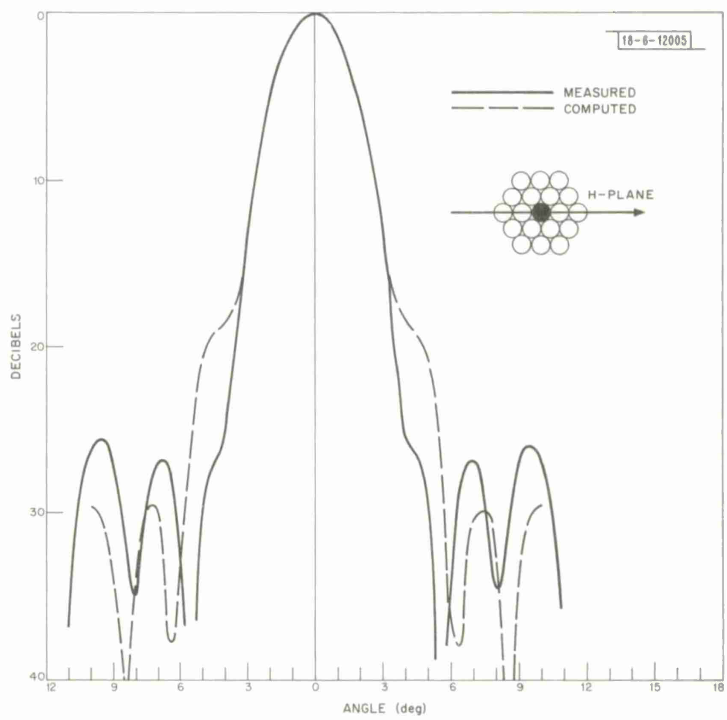

Fig. 15. Continued.

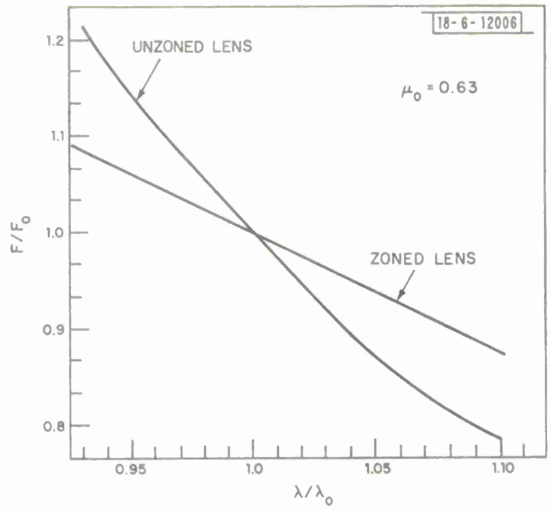

Fig. 16. Focal length of lens as a function of frequency.

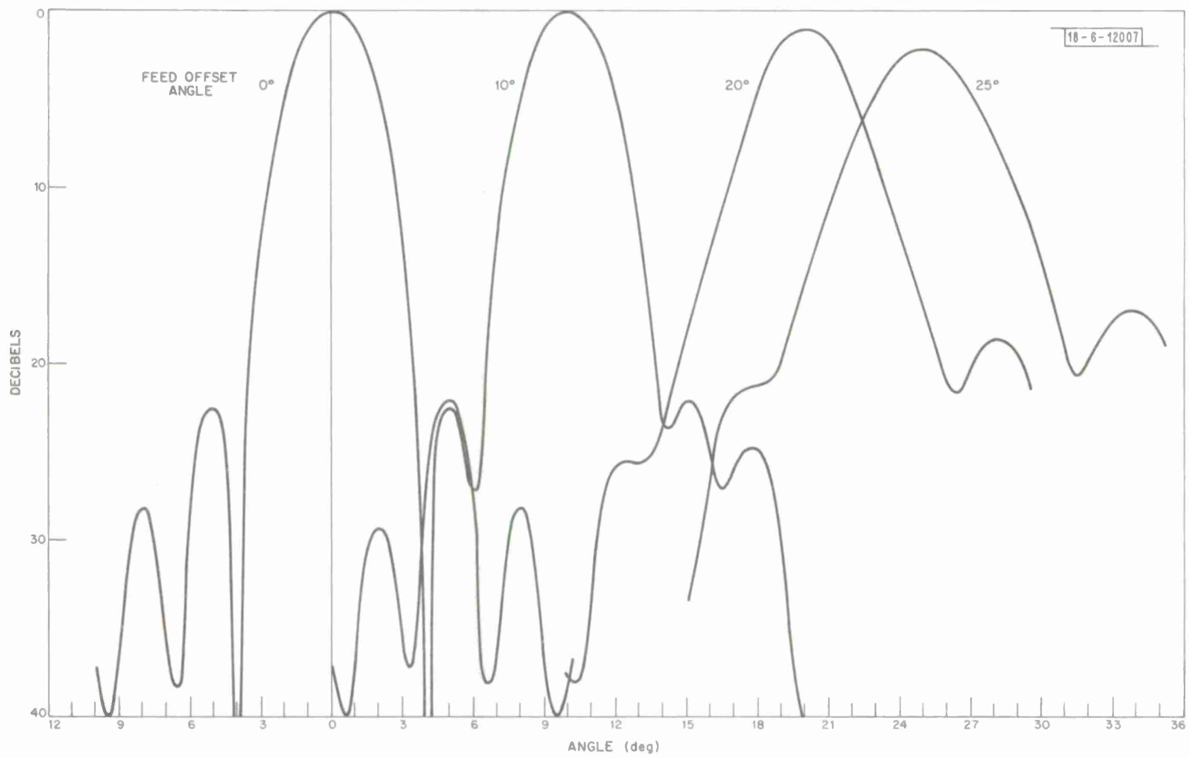

Fig. 17. Computed radiation patterns of double-concave lens for feed offset angles of 0°, 10°, 20°, and 25°.

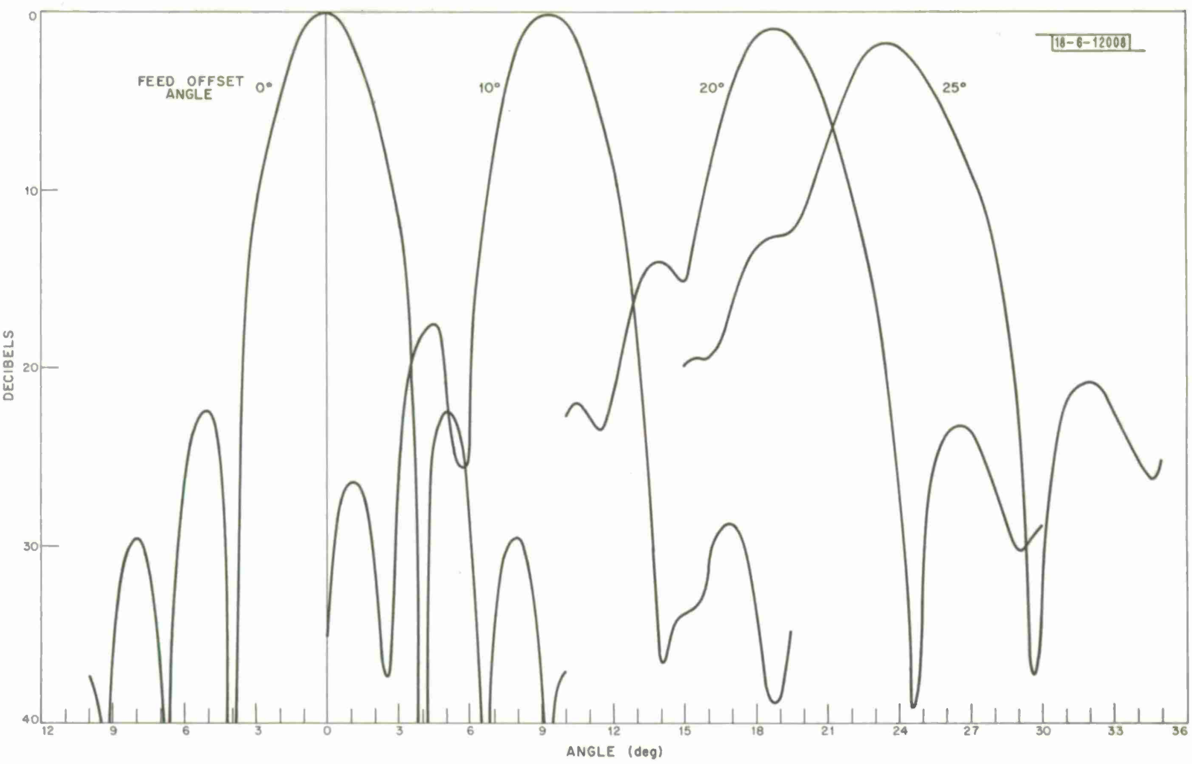

Fig. 18. Computed radiation patterns of plano-concave lens for feed offset angles of 0°, 10°, 20°, and 25°.

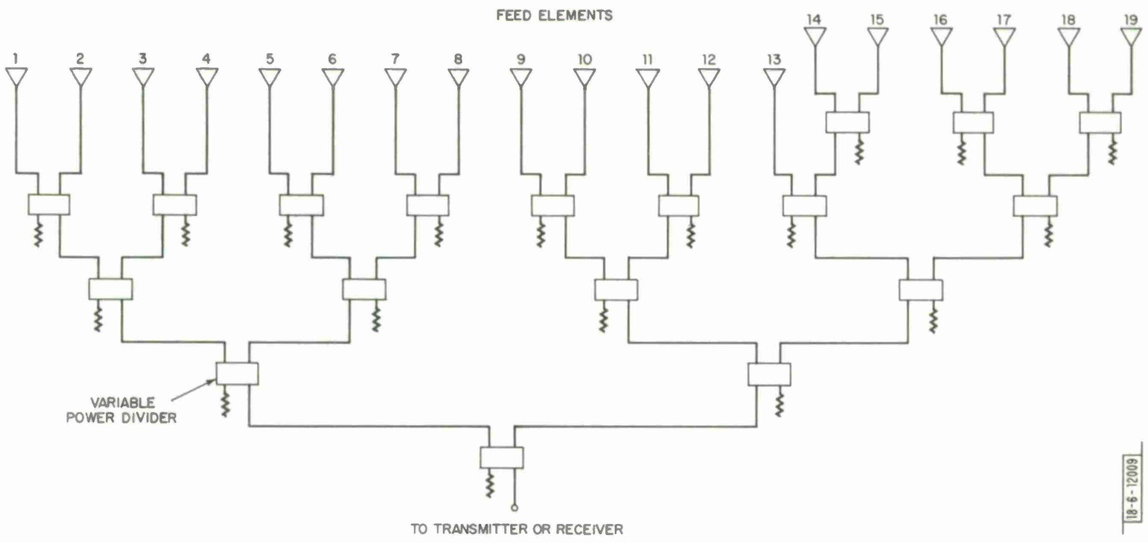

Fig. 19. Proposed combiner switch.

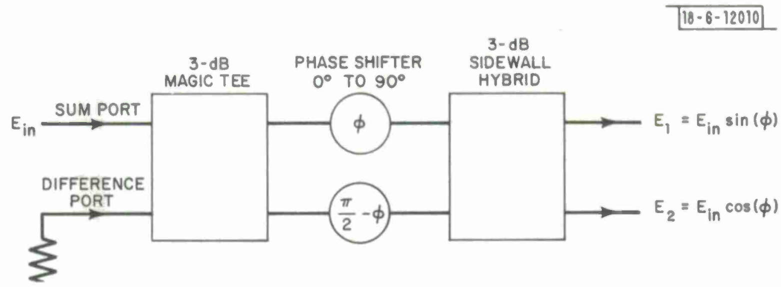

Fig. 20. Power divider.

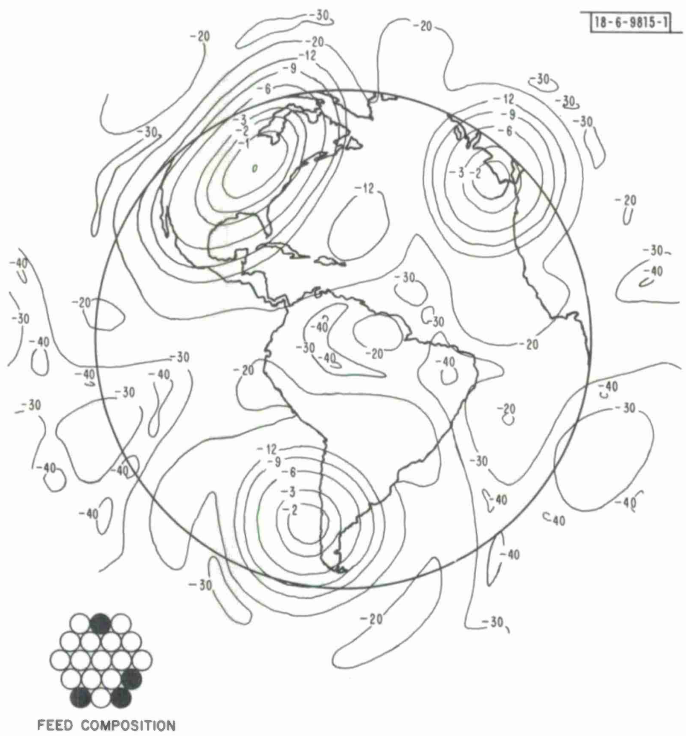

Fig. 21. Illustrating a compound coverage (measurements in decibels).

UNCLASSIFIED
Security Classification

DOCUMENT CONTROL DATA – R&D

(Security classification of title, body of abstract and indexing annotation must be entered when the overall report is classified)

1. ORIGINATING ACTIVITY *(Corporate author)* Lincoln Laboratory, M.I.T.	2a. REPORT SECURITY CLASSIFICATION Unclassified 2b. GROUP None

3. REPORT TITLE

Variable-Coverage Communications Antenna for LES-7

4. DESCRIPTIVE NOTES *(Type of report and inclusive dates)*

Technical Report

5. AUTHOR(S) *(Last name, first name, initial)*

Dion, Andre R.

6. REPORT DATE	7a. TOTAL NO. OF PAGES	7b. NO. OF REFS
17 October 1969	28	8

8a. CONTRACT OR GRANT NO. AF 19(628)-5167 b. PROJECT NO. 649L c. d.	9a. ORIGINATOR'S REPORT NUMBER(S) Technical Report 471 9b. OTHER REPORT NO(S) *(Any other numbers that may be assigned this report)* ESD-TR-69-319

10. AVAILABILITY/LIMITATION NOTICES

This document has been approved for public release and sale; its distribution is unlimited.

11. SUPPLEMENTARY NOTES	12. SPONSORING MILITARY ACTIVITY
None	Air Force Systems Command, USAF

13. ABSTRACT

An experimental model of the variable-coverage communications antenna system for the LES-7 spacecraft is described. Consisting of a waveguide lens, a 19-horn feed cluster, and a combiner switch, the system will permit selection of the antenna pattern that best matches a desired coverage on earth. The coverages realizable are of many sizes and shapes, and extend from that of a 3° pencil beam to a full hemisphere. A computer study of this antenna system gave results in good agreement with measurement. The salient features of this study are also described.

14. KEY WORDS

LES-7	X-band	shaped-beam antennas
communications antenna	Cassegrainian antennas	multiple-beam antenna
waveguide lens	antenna configurations	combiner switch

UNCLASSIFIED
Security Classification

Printed by
United States Air Force
L. G. Hanscom Field
Bedford, Massachusetts